

Arbitrary Reduction of MRI Inter-slice Spacing Using Hierarchical Feature Conditional Diffusion

Xin Wang^{1*}, Zhenrong Shen^{1*}, Zhiyun Song¹, Sheng Wang¹, Mengjun Liu¹,
Lichi Zhang¹, Kai Xuan², and Qian Wang³(✉)

¹ School of Biomedical Engineering, Shanghai Jiao Tong University, Shanghai, China

² School of Artificial Intelligence, Nanjing University of Information Science and Technology, Nanjing, China

³ School of Biomedical Engineering, ShanghaiTech University, Shanghai, China
qianwang@shanghaitech.edu.cn

Abstract. Magnetic resonance (MR) images collected in 2D scanning protocols typically have large inter-slice spacing, resulting in high in-plane resolution but reduced through-plane resolution. Super-resolution techniques can reduce the inter-slice spacing of 2D scanned MR images, facilitating the downstream visual experience and computer-aided diagnosis. However, most existing super-resolution methods are trained at a fixed scaling ratio, which is inconvenient in clinical settings where MR scanning may have varying inter-slice spacings. To solve this issue, we propose *Hierarchical Feature Conditional Diffusion (HiFi-Diff)* for arbitrary reduction of MR inter-slice spacing. Given two adjacent MR slices and the relative positional offset, HiFi-Diff can iteratively convert a Gaussian noise map into any desired in-between MR slice. Furthermore, to enable fine-grained conditioning, the Hierarchical Feature Extraction (HiFE) module is proposed to hierarchically extract conditional features and conduct element-wise modulation. Our experimental results on the publicly available HCP-1200 dataset demonstrate the high-fidelity super-resolution capability of HiFi-Diff and its efficacy in enhancing downstream segmentation performance.

Keywords: Magnetic Resonance Imaging · Super-resolution · Diffusion Model · Conditional Image Synthesis

1 Introduction

Magnetic resonance imaging (MRI) is essential for analyzing and diagnosing various diseases, owing to its non-invasive property and superior contrast for soft tissues. In clinical practice, 2D scanning protocols are commonly employed for MR image acquisition due to limitations in scanning time and signal-to-noise ratio. Typically, such scanning protocols produce MR volumes with small intra-slice spacing but much larger inter-slice spacing, which poses a great challenge for many volumetric image processing toolkits [5,13] that require near-isotropic

* Contributed equally to this work.

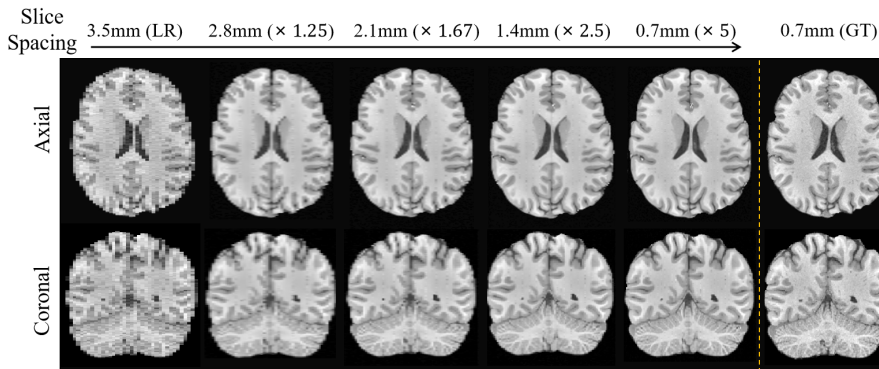


Fig. 1. A test case of applying HiFi-Diff to arbitrary reduction of MR inter-slice (sagittal) spacing. The visual quality of the resulting images in the axial and coronal views is gradually enhanced with increasing SR factors.

voxel spacing of the input images. Therefore, it is necessary to resample the acquired volumes to align the inter-slice spacing with the intra-slice spacing.

Interpolation methods are widely used to reduce the inter-slice spacing of 2D scanned MR volumes. However, these methods simply calculate missing voxels as a weighted average of the adjacent ones, leading to inevitable blurred results. For better performance, many deep-learning-based super-resolution (SR) studies have been investigated [7,1,2,21,12]. In this paper, we term large slice spacing as *low resolution* (LR) and small slice spacing as *high resolution* (HR). DeepResolve [1] adopts a 3D convolutional network to obtain HR images from LR ones, but it only considers reducing inter-slice spacing at a fixed ratio. Training such an SR model for each scaling ratio is impractical, as it requires significant time and computational resources.

To tackle this issue, local implicit image function (LIIF) [2] and MetaSR [12] are proposed to perform arbitrary-scale SR for natural images. To achieve arbitrary-scale SR of MR images, ArSSR [21] extends LIIF to 3D volumes and utilizes a continuous implicit voxel function for reconstructing HR images at different ratios. Although ArSSR produces competitive quantitative results, it still suffers from image over-smoothing. To solve the aforementioned problem, adversarial learning [9] is usually introduced to synthesize more image details. However, such a training scheme often leads to training instability and is prone to generate artifacts [18,6].

Recently, diffusion models [19,11] have achieved wide success in image synthesis tasks, outperforming other deep generative models in terms of visual fidelity and training stability. Typical denoising diffusion models (*e.g.*, DDPM [11]) use a series of denoising operations to iteratively generate samples from a prior distribution (*e.g.*, Gaussian) to a desired data distribution. Although there exist several works that apply diffusion models for MR image reconstruction [4] or

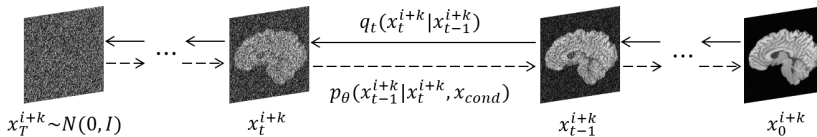


Fig. 2. Conditional diffusion process of HiFi-Diff, where q_t and p_θ denote single-step transitions in forward and reverse processes, respectively.

denoising [3], the application of diffusion models to achieve arbitrary-scale MR image super-resolution has not been studied yet.

In this paper, by leveraging the powerful ability of the diffusion models, we propose *Hierarchical Feature Conditional Diffusion (HiFi-Diff)*, which allows arbitrary reduction of inter-slice spacing for 2D scanned MR images, as shown in Fig. 1. Conditioned on two adjacent LR slices, HiFi-Diff can generate any in-between MR slices. To handle different ratios of inter-slice spacing, we construct continuous representations for the spatial positions between two adjacent LR slices by providing relative positional offsets as additional conditions. Inspired by the core idea of FPN [15], we propose the Hierarchical Feature Extraction (HiFE) module, which applies different-scale feature maps as conditions to perform element-wise feature modulation in each layer. The experimental results demonstrate that HiFi-Diff produces MR slices of excellent quality and effectively enhances downstream image segmentation tasks.

In summary, the main contributions of this paper include: (1) To the best of our knowledge, HiFi-Diff is the first diffusion model for arbitrary-scale SR of MR images. (2) We propose the HiFE module to hierarchically extract conditional features for fine-grained conditioning on MR slice generation.

2 Method

We discuss the conditional diffusion process and the network architecture of HiFi-Diff in Section 2.1 and Section 2.2, respectively.

2.1 Conditional Diffusion for Arbitrary-scale Super-resolution

Let $x_0^i \in \mathbb{R}^{H \times W}$ denote a sample from 2D MR slice distribution, where the subscript 0 refers to the initial timestep and the superscript i refers to the slice index. For arbitrary-scale SR, we aim to learn continuous representations for the spatial positions between any two adjacent MR slices in an LR volume. Specifically, we define the generated slice between x_0^i and x_0^{i+1} as x_0^{i+k} , where $k \in [0, 1]$ is a non-integral offset denoting its relative distance to x_0^i .

Similar to DDPM [11], HiFi-Diff learns a Markov chain process to convert the Gaussian distribution into the target data distribution, as demonstrated in Fig. 2. The forward diffusion process gradually adds Gaussian noises ϵ_t to the

target MR slice x_0^{i+k} according to a variance schedule β_t from $t = 0$ to $t = T$, which can be represented as:

$$q_t(x_t^{i+k}|x_{t-1}^{i+k}) = \mathcal{N}(x_t^{i+k}; \sqrt{1 - \beta_t}x_{t-1}^{i+k}, \beta_t\mathbf{I}), \quad (1)$$

Furthermore, we can directly sample x_t^{i+k} from x_0^{i+k} at an arbitrary timestep t in a closed form using the following accumulated expression:

$$q_t(x_t^{i+k}|x_0^{i+k}) = \mathcal{N}(x_t^{i+k}; \sqrt{\bar{\alpha}_t}x_0^{i+k}, (1 - \bar{\alpha}_t)\mathbf{I}) \Rightarrow x_t^{i+k} = \sqrt{\bar{\alpha}_t}x_0^{i+k} + (1 - \bar{\alpha}_t)\epsilon, \quad (2)$$

where $\bar{\alpha}_t = \prod_{s=1}^t(1 - \beta_s)$ and $\epsilon \sim \mathcal{N}(\mathbf{0}, \mathbf{I})$. To gain the generation ability for MR slices, HiFi-Diff learns the reverse diffusion via a parameterized Gaussian process $p_\theta(x_{t-1}^{i+k}|x_t^{i+k}, x_{cond})$ conditioned on the feature pyramid x_{cond} :

$$p_\theta(x_{t-1}^{i+k}|x_t^{i+k}, x_{cond}) = \mathcal{N}(x_{t-1}^{i+k}; \mu_\theta(x_t^{i+k}, t, x_{cond}), \sigma_t^2\mathbf{I}), \quad (3)$$

where σ_t^2 is a fixed variance and $\mu_\theta(x_t^{i+k}, t, x_{cond})$ is a learned mean defined as:

$$\mu_\theta(x_t^{i+k}, t, x_{cond}) = \frac{1}{\sqrt{1 - \beta_t}} \left(x_t^{i+k} - \frac{\beta_t}{\sqrt{1 - \bar{\alpha}_t}} \epsilon_\theta(x_t^{i+k}, t, x_{cond}) \right) \quad (4)$$

where $\epsilon_\theta(x_t^{i+k}, t, x_{cond})$ denotes the main branch of HiFi-Diff for noise prediction. To generate in-between slices x_0^{i+k} , we iteratively compute the denoising process $x_{t-1}^{i+k} = \mu_\theta(x_t^{i+k}, t, x_{cond}) + \sigma_t z$, where $z \sim \mathcal{N}(\mathbf{0}, \mathbf{I})$.

HiFi-Diff is trained in an end-to-end manner by optimizing the simple variant of the variational lowerbound \mathcal{L}_{simple} with respect to θ and ϕ :

$$\begin{aligned} \mathcal{L}_{simple}(\theta, \phi) &= \mathbb{E}_{x_0^{i+k}, t, x_{cond}} \left[\left\| \epsilon_\theta(x_t^{i+k}, t, x_{cond}) - \epsilon_t \right\|_2^2 \right] \\ &= \mathbb{E}_{x_0^{i+k}, t, x_0^i, x_0^{i+1}, k} \left[\left\| \epsilon_\theta(x_t^{i+k}, t, \mathcal{F}_\phi(x_0^i, x_0^{i+1}, k)) - \epsilon_t \right\|_2^2 \right], \end{aligned} \quad (5)$$

where \mathcal{F}_ϕ parameterizes the proposed HiFE module, ϵ_t is the Gaussian distribution data with $\mathcal{N}(\mathbf{0}, \mathbf{I})$, and t is a timestep uniformly sampled from $[0, T]$.

2.2 Hierarchical Feature Conditioning Framework

Given any pair of x_0^i and x_0^{i+1} from an LR volume with a desired offset k , HiFi-Diff is able to iteratively convert a Gaussian noise map into the target in-between slice x_0^{i+k} through a reversed diffusion process, as described in the last section.

In this section, we introduce the network architecture of HiFi-Diff. As illustrated in Fig. 3(a), the adjacent MR slices x_0^i and x_0^{i+1} are concatenated and input to the proposed HiFE module, which adopts a U-Net [17] architecture consisting of a stack of residual blocks (shown in Fig. 3(b)). The offset k is injected into each residual block to perform channel-wise modulation. Specifically, k is projected by two successive fully connected layers into a 128-dimensional

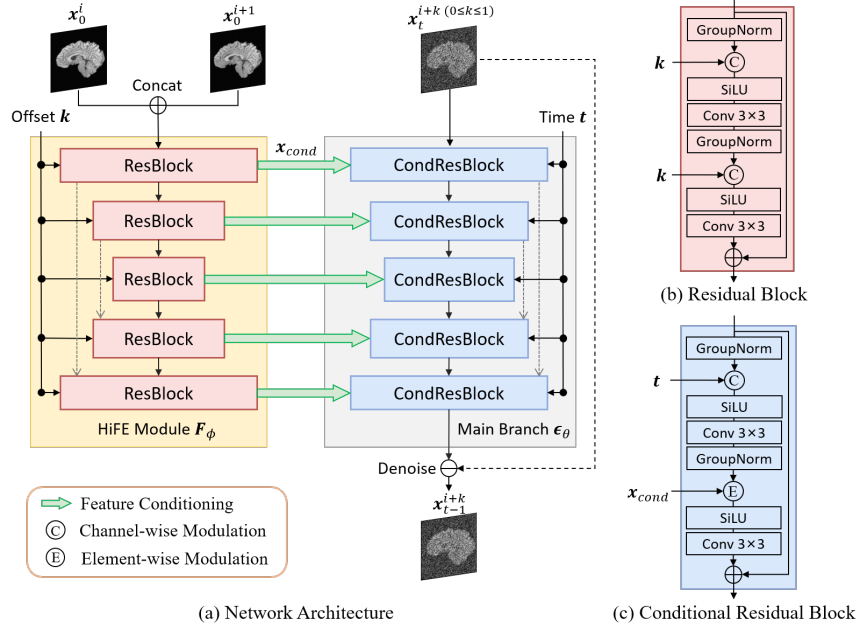


Fig. 3. Overview of *Hierarchical Feature Conditional Diffusion (HiFi-Diff)*.

index embedding. Next, for each layer, the index embedding is passed through a learnable affine transformation to obtain the channel-wise scaling and bias parameters (k_s, k_b) , which are applied to the feature map h using the expression $\text{ChannelMod}(h, k_s, k_b) = k_s \text{GroupNorm}(h) + k_b$. In this way, the HiFE module yields an hourglass-like feature hierarchy that includes feature maps at different scales, with semantics ranging from low to high levels.

Conditioned on the timestep t and the feature pyramid x_{cond} , the main branch of HiFi-Diff learns to gradually denoise the noise-corrupted input slice x_t^{i+k} . The main branch has the same U-Net architecture as HiFE module and consists of a stack of conditional residual blocks. For each conditional residual block (shown in Fig. 3(c)) in the main branch, the timestep t performs channel-wise modulation in the same way that the offset k does in each residual block of HiFE module. After the channel-wise modulation, the feature map is further modulated by x_{cond} from the lateral connection at the same image level. The conditional feature x_{cond} is transformed into the scaling and bias parameters (x_s, x_b) that have the same spatial sizes as the feature map h , such that x_{cond} can shift group-normalized h in an element-wise manner: $\text{ElementMod}(h, x_s, x_b) = x_s \text{GroupNorm}(h) + x_b$. Through element-wise modulation, the hierarchical feature pyramid x_{cond} provides fine-grained conditioning to guide the MR slice generation.

Table 1. Quantitative comparison of $\times 4$, $\times 5$, $\times 6$, and $\times 7$ SR tasks between the proposed HiFi-Diff and other SR methods.

Task	Method	PSNR	SSIM	Dice	
				WM	GM
$\times 4$	Interpolation	36.05 \pm 2.394	0.9758 \pm 0.0070	0.9112 \pm 0.0084	0.7559 \pm 0.0177
	DeepResolve	39.65 \pm 2.281	0.9880 \pm 0.0039	0.9700 \pm 0.0021	0.9230 \pm 0.0055
	MetaSR	39.30 \pm 2.287	0.9876 \pm 0.0039	0.9672 \pm 0.0027	0.9152 \pm 0.0065
	ArSSR	39.65 \pm 2.282	0.9884 \pm 0.0037	0.9687 \pm 0.0026	0.9171 \pm 0.0067
	w/o HiFE	38.78 \pm 2.298	0.9874 \pm 0.0039	0.9639 \pm 0.0033	0.9118 \pm 0.0078
	HiFi-Diff	39.50 \pm 2.285	0.9890 \pm 0.0040	0.9700 \pm 0.0045	0.9229 \pm 0.0057
$\times 5$	Interpolation	31.55 \pm 2.381	0.9542 \pm 0.0113	0.8362 \pm 0.0090	0.6470 \pm 0.0136
	DeepResolve	38.28 \pm 2.318	0.9848 \pm 0.0047	0.9617 \pm 0.0028	0.9006 \pm 0.0070
	MetaSR	37.95 \pm 2.279	0.9840 \pm 0.0049	0.9522 \pm 0.0043	0.8808 \pm 0.0100
	ArSSR	38.27 \pm 2.261	0.9850 \pm 0.0045	0.9552 \pm 0.0039	0.8847 \pm 0.0100
	w/o HiFE	37.53 \pm 2.289	0.9832 \pm 0.0051	0.9538 \pm 0.0042	0.8827 \pm 0.0109
	HiFi-Diff	38.25 \pm 2.260	0.9852 \pm 0.0047	0.9620 \pm 0.0060	0.9007 \pm 0.0104
$\times 6$	Interpolation	30.44 \pm 2.379	0.9457 \pm 0.0129	0.7967 \pm 0.0111	0.5749 \pm 0.0159
	DeepResolve	37.21 \pm 2.315	0.9814 \pm 0.0055	0.9521 \pm 0.0033	0.8786 \pm 0.0078
	MetaSR	36.55 \pm 2.286	0.9792 \pm 0.0061	0.9286 \pm 0.0066	0.8298 \pm 0.0142
	ArSSR	36.62 \pm 2.271	0.9798 \pm 0.0058	0.9330 \pm 0.0061	0.8358 \pm 0.0141
	w/o HiFE	36.67 \pm 2.292	0.9801 \pm 0.0058	0.9414 \pm 0.0042	0.8569 \pm 0.0097
	HiFi-Diff	37.41 \pm 2.314	0.9827 \pm 0.0054	0.9527 \pm 0.0111	0.8798 \pm 0.0169
$\times 7$	Interpolation	29.61 \pm 2.379	0.9386 \pm 0.0142	0.7611 \pm 0.0130	0.5144 \pm 0.0185
	DeepResolve	36.35 \pm 2.303	0.9782 \pm 0.0063	0.9387 \pm 0.0046	0.8468 \pm 0.0104
	MetaSR	35.27 \pm 2.308	0.9739 \pm 0.0074	0.8988 \pm 0.0092	0.7691 \pm 0.0180
	ArSSR	35.20 \pm 2.289	0.9741 \pm 0.0072	0.9034 \pm 0.0090	0.7739 \pm 0.0192
	w/o HiFE	35.86 \pm 2.316	0.9766 \pm 0.0070	0.9245 \pm 0.0056	0.8254 \pm 0.0122
	HiFi-Diff	36.58 \pm 2.328	0.9797 \pm 0.0062	0.9401 \pm 0.0103	0.8550 \pm 0.0177

3 Experimental Results

3.1 Dataset and Experimental Setup

Data Preparation We collect 1,113 subjects of 3T MR images from the HCP-1200 dataset [8], with all images having an isotropic voxel spacing of 0.7mm \times 0.7mm \times 0.7mm. Among these, 891 images are used for training, and the remaining 222 images are used for testing. We perform N4 bias correction and skull-stripping for preprocessing. It is noteworthy that skull-stripping is necessary in order to protect the privacy of the subjects. To simulate the LR images with large slice spacing, we downsample the isotropic HR volumes perpendicular to the sagittal view following [1].

Implementation Details To achieve a comprehensive evaluation, we compare HiFi-Diff with other methods for MR super-resolution, including trilinear interpolation, DeepResolve [1], MetaSR [12], and ArSSR [21]. DeepResolve is trained and tested for each specific scaling ratio, while HiFi-Diff, MetaSR, and ArSSR are trained using mixed scaling ratios of $\times 2$, $\times 3$, $\times 4$ for arbitrary-scale super-resolution. In each iteration of training, we corrupt the intermediate slice

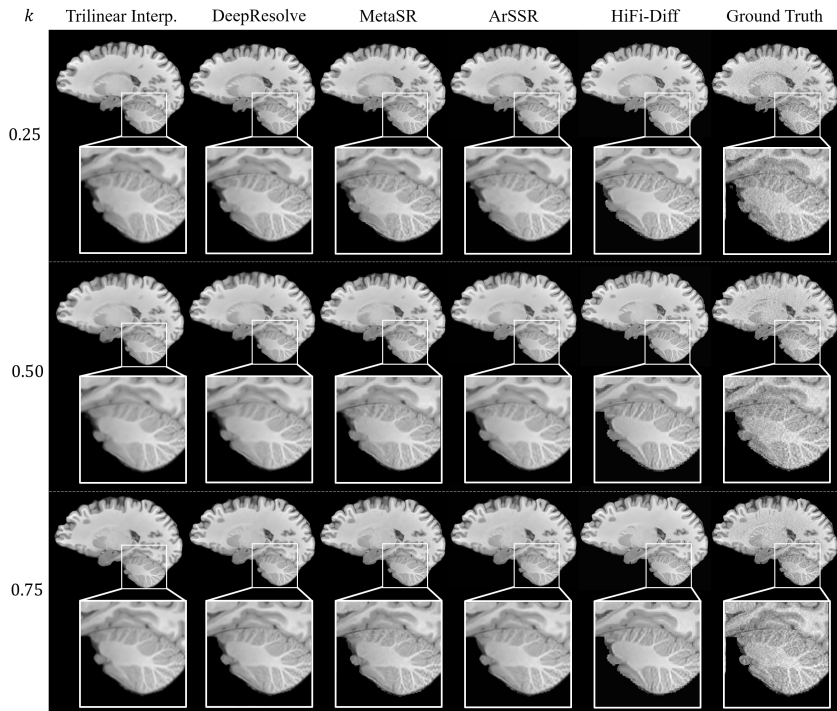


Fig. 4. Qualitative comparison of $\times 4$ SR task between the proposed HiFi-Diff and other SR methods. The cerebellum regions are highlighted and zoomed in.

x_0^{i+k} with Gaussian noise according to the randomly sampled timestep t . We set $T = 1000$ during training, and use DDIM sampler [20] to speed up the reverse process by reducing $T = 1000$ to $T = 100$. All the experiments are conducted using an NVIDIA A100 40G with PyTorch [16]. We use the learning rate of 1.0×10^{-4} , batch size of 1, and Adam optimizer [14] to train our model for 700k iterations.

3.2 Super-resolution Evaluation

We use Peak Signal-to-Noise Ratio (PSNR) and Structural Similarity Index (SSIM) to evaluate the consistency between the SR results and ground truth. Based on the results in Table 1, the proposed HiFi-Diff method outperforms other state-of-the-art methods, particularly at large scaling ratios. It is worth mentioning that DeepResolve achieves the highest PSNR scores at scaling ratios of $\times 4$ and $\times 5$, which can be attributed to the fact that DeepResolve is specifically trained for each scaling ratio.

In addition, we conduct an ablation study to assess the effectiveness of the HiFE module by removing it and comparing the results. In detail, we directly

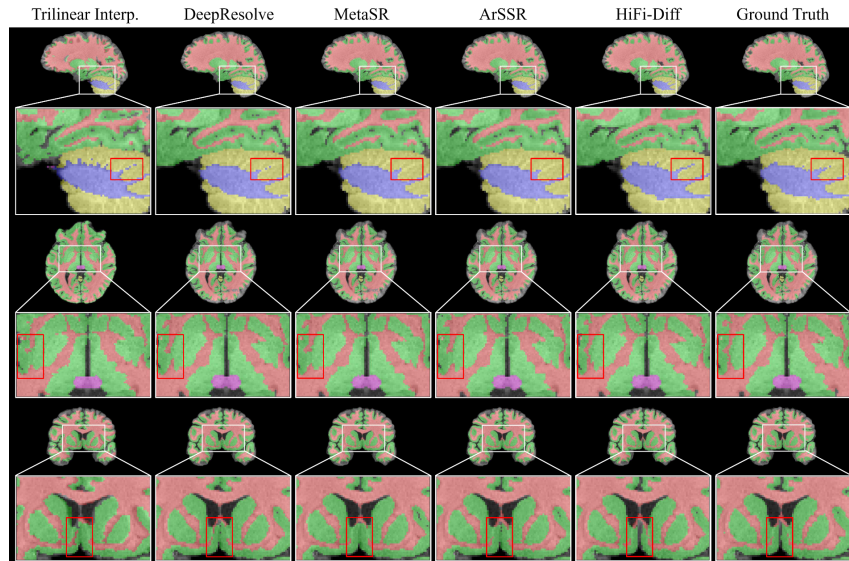


Fig. 5. Visual comparison of the fully automatic segmentation on $\times 4$ SR results by all the comparing models. The sagittal, axial, and coronal views are shown in three rows, respectively. The areas surrounded by the white boxes are zoomed in below.

inject the concatenated slices into the main branch for element-wise modulation, and concatenate the embedding of offset k and timestep t for channel-wise modulation. The results show a decrease in all metrics when the HiFE module is removed, indicating that HiFi-Diff benefits from the fine-grained conditioning provided by the HiFE module.

The qualitative comparison of the generated in-between MR slices with different offsets is shown in Fig. 4. By inspection of the cerebellum, one can notice that other methods fail to produce complete and clear structures of the white matter for they are optimized using L1/L2 loss, driving their results towards over-smoothing and loss of high-frequency information. In contrast, HiFi-Diff can faithfully reconstruct image details through an iterative diffusion process.

To validate the effectiveness of the proposed HiFi-Diff on downstream tasks, we conduct brain segmentation on different SR results using Fastsurfer [10]. According to Table 1, HiFi-Diff outperforms other methods in terms of Dice score for the white matter (WM) and the gray matter (GM) in most scenarios. The visual comparison in Fig. 5 further demonstrates the superiority of HiFi-Diff, as other methods yield tissue adhesion or discontinuity in their segmented results, while our approach avoids these problems.

4 Conclusion and Discussion

In conclusion, we propose HiFi-Diff to conduct arbitrary reduction of MR interslice spacing, outperforming previous methods in both generation capability and downstream task performance by leveraging the power of the diffusion models. To further enhance fine-grained conditioning, we introduce the HiFE module, which hierarchically extracts conditional features and conducts element-wise feature modulations. Despite the superior performance, HiFi-Diff still suffers from slow sampling speed. One possible solution is the implementation of faster sampling algorithms or the utilization of techniques such as knowledge distillation.

References

1. Chaudhari, A.S., Fang, Z., Kogan, F., Wood, J., Stevens, K.J., Gibbons, E.K., Lee, J.H., Gold, G.E., Hargreaves, B.A.: Super-resolution musculoskeletal mri using deep learning. *Magnetic resonance in medicine* **80**(5), 2139–2154 (2018)
2. Chen, Y., Liu, S., Wang, X.: Learning continuous image representation with local implicit image function. In: 2021 IEEE/CVF Conference on Computer Vision and Pattern Recognition (CVPR). pp. 8624–8634 (2021). <https://doi.org/10.1109/CVPR46437.2021.00852>
3. Chung, H., Lee, E.S., Ye, J.C.: Mr image denoising and super-resolution using regularized reverse diffusion. *IEEE Transactions on Medical Imaging* (2022)
4. Cui, Z.X., Cao, C., Liu, S., Zhu, Q., Cheng, J., Wang, H., Zhu, Y., Liang, D.: Self-score: Self-supervised learning on score-based models for mri reconstruction. arXiv preprint arXiv:2209.00835 (2022)
5. Desikan, R.S., Ségonne, F., Fischl, B., Quinn, B.T., Dickerson, B.C., Blacker, D., Buckner, R.L., Dale, A.M., Maguire, R.P., Hyman, B.T., Albert, M.S., Killiany, R.J.: An automated labeling system for subdividing the human cerebral cortex on mri scans into gyral based regions of interest. *NeuroImage* **31**(3), 968 – 980 (2006). <https://doi.org/DOI: 10.1016/j.neuroimage.2006.01.021>
6. Dhariwal, P., Nichol, A.: Diffusion models beat gans on image synthesis. *Advances in Neural Information Processing Systems* **34**, 8780–8794 (2021)
7. Dong, C., Loy, C.C., He, K., Tang, X.: Image super-resolution using deep convolutional networks. *IEEE Transactions on Pattern Analysis and Machine Intelligence* **38**(2), 295–307 (2016). <https://doi.org/10.1109/TPAMI.2015.2439281>
8. Glasser, M.F., Sotiropoulos, S.N., Wilson, J.A., Coalson, T.S., Fischl, B., Andersson, J.L., Xu, J., Jbabdi, S., Webster, M., Polimeni, J.R., Van Essen, D.C., Jenkinson, M.: The minimal preprocessing pipelines for the human connectome project. *NeuroImage* **80**, 105–124 (2013), mapping the Connectome
9. Goodfellow, I., Pouget-Abadie, J., Mirza, M., Xu, B., Warde-Farley, D., Ozair, S., Courville, A., Bengio, Y.: Generative adversarial networks. *Communications of the ACM* **63**(11), 139–144 (2020)
10. Henschel, L., Conjeti, S., Estrada, S., Diers, K., Fischl, B., Reuter, M.: Fastsurfer—a fast and accurate deep learning based neuroimaging pipeline. *NeuroImage* **219**, 117012 (2020)
11. Ho, J., Jain, A., Abbeel, P.: Denoising diffusion probabilistic models. *Advances in Neural Information Processing Systems* **33**, 6840–6851 (2020)

12. Hu, X., Mu, H., Zhang, X., Wang, Z., Tan, T., Sun, J.: Meta-sr: A magnification-arbitrary network for super-resolution. In: 2019 IEEE/CVF Conference on Computer Vision and Pattern Recognition (CVPR). pp. 1575–1584 (2019). <https://doi.org/10.1109/CVPR.2019.00167>
13. Jenkinson, M., Beckmann, C.F., Behrens, T.E., Woolrich, M.W., Smith, S.M.: Fsl. *NeuroImage* **62**(2), 782–790 (2012). <https://doi.org/https://doi.org/10.1016/j.neuroimage.2011.09.015>, <https://www.sciencedirect.com/science/article/pii/S1053811911010603>, 20 YEARS OF fMRI
14. Kingma, D.P., Ba, J.: Adam: A method for stochastic optimization (2014), cite arxiv:1412.6980Comment: Published as a conference paper at the 3rd International Conference for Learning Representations, San Diego, 2015
15. Lin, T.Y., Dollár, P., Girshick, R., He, K., Hariharan, B., Belongie, S.: Feature pyramid networks for object detection. In: Proceedings of the IEEE conference on computer vision and pattern recognition. pp. 2117–2125 (2017)
16. Paszke, A., Gross, S., Chintala, S., Chanan, G., Yang, E., DeVito, Z., Lin, Z., Desmaison, A., Antiga, L., Lerer, A.: Automatic differentiation in pytorch. In: NIPS 2017 Workshop on Autodiff (2017)
17. Ronneberger, O., Fischer, P., Brox, T.: U-net: Convolutional networks for biomedical image segmentation. In: Medical Image Computing and Computer-Assisted Intervention–MICCAI 2015: 18th International Conference, Munich, Germany, October 5–9, 2015, Proceedings, Part III 18. pp. 234–241. Springer (2015)
18. Salimans, T., Goodfellow, I.J., Zaremba, W., Cheung, V., Radford, A., Chen, X.: Improved techniques for training gans. *CoRR* **abs/1606.03498** (2016), <http://arxiv.org/abs/1606.03498>
19. Sohl-Dickstein, J., Weiss, E., Maheswaranathan, N., Ganguli, S.: Deep unsupervised learning using nonequilibrium thermodynamics. In: International Conference on Machine Learning. pp. 2256–2265. PMLR (2015)
20. Song, J., Meng, C., Ermon, S.: Denoising diffusion implicit models. *arXiv preprint arXiv:2010.02502* (2020)
21. Wu, Q., Li, Y., Sun, Y., Zhou, Y., Wei, H., Yu, J., Zhang, Y.: An arbitrary scale super-resolution approach for 3-dimensional magnetic resonance image using implicit neural representation (2021)